e-Navi

Available online at http://www.e-navigation.kr/
e-Navigation Journal

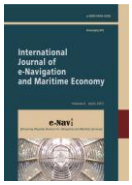

Original article

Combined Effect of Suction Intensity and Suction Port Position on the Aerodynamic Characteristics of Suction-Type Turbine Sail

Deqi Jiang[a] , Haihua Lin[b], Chengmeng Sun[c]

[a] School of Naval Architecture and Port Engineering, Shandong Jiaotong University, Weihai 264209, China, 1715012465@qq.com

[b] School of Naval Architecture and Port Engineering, Shandong Jiaotong University, Weihai 264209, China, 7216219@qq.com

[C] School of Naval Architecture and Port Engineering, Shandong Jiaotong University, Weihai 264209, China, scmeng717@163.com , Corresponding Author

Abstract

With the increasing demand for energy conservation and emissions reduction in the shipping industry, suction-based turbine sails have emerged as a novel wind energy utilization technology and have become a research hotspot. This study focuses on the aerodynamic performance of suction-based turbine sails with the aim of investigating the effects of suction intensity and suction port position on their aerodynamic characteristics. By employing Computational Fluid Dynamics (CFD) numerical simulations using the Re-Normalization Group (RNG) k–ε turbulence model and the SIMPLE algorithm, this study provides a detailed analysis of lift and drag coefficients, pressure distribution, and vorticity distribution under various combinations of suction intensity (γ) and suction port position (α). The results show that variations in suction intensity significantly affect the lift and drag characteristics of the turbine sail, while changes in the suction port position directly influence the attachment and separation behavior of airflow on the sail surface. Furthermore, a synergistic effect is observed between γ and α—their interaction not only alters the flow distribution but also plays a critical role in determining the overall performance of the turbine sail.By comprehensively considering the influence of these two factors, the study draws key conclusions for optimizing the design of suction-based turbine sail, providing valuable theoretical insights and technical guidance for their practical application in wind-assisted marine propulsion.

Keywords: Turbine Sail, Suction Port Position , Suction Intensity, Numerical Simulations

https://doi.org/10.52820/j.enavi.2025.24.001

1. Introduction

In the context of global energy saving, emissions reduction, and sustainable development, exploring innovative energy utilization methods has become a key task for achieving green development and addressing climate change (2024) (2024). The shipping industry is one of the major sectors responsible for energy consumption and greenhouse gas emissions, making the search for efficient and environmentally friendly wind-assisted propulsion technologies crucial for improving energy utilization efficiency and reducing carbon emissions (^{0}2024) (2024). The suction-type turbine sail, an emerging wind-assisted propulsion device utilizing suction control technology, has the potential to provide new breakthroughs in energy saving and emission reduction for ships.

In recent years, the application of suction control technology has significantly increased. In bridges and structural vibrations, suction technology can reduce the longitudinal and transverse amplitudes of cable vibrations and lower noise levels (2023) (2024). In submarine navigation, suction technology can suppress turbulence noise by altering wake characteristics (2020)^{0}. In addition, suction technology has been successfully applied to the flow around cylindrical bodies. For example, in flow fields around cylindrical and square column structures, suction technology has been shown to significantly reduce fluid resistance, suppress vortex-induced vibrations and vortex shedding phenomena, reduce wake vibrations, and improve structural stability (2021) (2016) (1994). Fransson J et al. (2004) found that uniform suction can significantly delay flow separation on the surface of a cylinder and move the separation point to the rear, effectively reducing drag. W. Chen et al. (2013) (2023) further found through wind tunnel experiments that optimizing suction flow rate can maximize the suppression of vortex-induced vibrations at low wind speeds. They also experimentally verified that distributed suction applied to the sidewall of a square column significantly suppressed the shear layer separation and reduced the vibration of unsteady wake flows. C. Liu (2017) used PIV experiments and CFD simulations to reveal the specific control mechanisms of suction on blunt body flow fields and found that suction not only significantly reduced the vortex strength and turbulence kinetic energy but also optimized the flow field structure and aerodynamic performance by altering the surface pressure distribution and delaying the separation point. Y Zhong et al. (2022) (2022) further revealed the optimization effects of suction angle and intensity on the wake of a cylinder through Particle Image Velocimetry (PIV) and numerical simulations, finding that suction could narrow the wake width and reduce the size of the recirculation zone. They also found that the distribution of the suction port positions significantly affects the scale and intensity of the Kármán vortices. These studies, which used wind tunnel experiments, PIV, and CFD simulations, have provided in-depth insights into the practical effects of suction control technology. They provided essential evidence for understanding the mechanisms of suction control and optimization of suction parameters.

With the continuous development of research and technology, significant progress has been made in applying suction technology to optimize airfoil aerodynamic performance. Researchers have thoroughly explored the impact of suction port position and size on aerodynamic performance. L. Wang et al. (2022). found that placing suction ports at the chord position of the NACA0012 airfoil could significantly delay the stall angle, increase the lift coefficient by 45%, and reduce the drag coefficient by 29%. W Zhang et al. (2017) further revealed through numerical simulations that the best effect of placing suction ports at 10%-20% of the leading-edge chord length not only improved aerodynamic performance but also delayed the stall angle to 20°, significantly reducing energy loss. Ma et al. (2018) found that positioning the suction ports near the laminar separation bubble could effectively control the boundary layer separation and improve the lift-to-drag ratio. S. Gao (2017) further pointed out that optimizing the size of suction ports can delay the flow separation on the airfoil surface, thereby improving the lift-to-drag ratio. These research results have had positive impacts on the application of suction control technology, promoting the development and innovation of related technologies and providing strong support for the wider application of suction control technology in various fields.

Furthermore, suction technology can be combined with blowing technology to form an efficient synergistic control strategy that can significantly enhance the aerodynamic performance of structures. This was

demonstrated by the improved suction and blowing system (IBSS) proposed by Balaji et al (2021). By placing blowing holes at the maximum thickness of the wing and suction holes near the trailing edge, they successfully delayed the stall angle and further increased the lift coefficient, while reducing turbulence noise on the wing surface. A. Farhadi et al. (2017) and И Корнилов et al. (2020) studied the effect of the combined suction and blowing action on the lift-to-drag ratio of airfoils, finding that optimizing the blowing parameters significantly improved the lift-to-drag ratio. K Dohyun et al. (2024) explored the combined application of suction and blowing in a multi-cylinder array, finding that suction stabilized the wake and reduced turbulence, enhancing the stability and efficiency of the propulsion. W Chen et al. (2020) further revealed the unique advantages of suction at the leading edge combined with blowing at the trailing edge in suppressing vortex shedding and enhancing flow field stability. This finding provides new perspectives and ideas for innovation in flow-control technologies.

Thus, suction-control technology has been widely applied in multiple fields. Notably, suction technology has demonstrated considerable application potential in the field of ship propulsion. Studies by C James et al (2021). and O Guerri et al. (2016). have confirmed this, suggesting that introducing suction control technology into wind-assisted propulsion systems can significantly improve the pressure distribution in the flow field, significantly enhance the lift-to-drag ratio, and effectively reduce the strength of vortex shedding. M Ghorbani et al. (2024) conducted a performance evaluation of suction-based turbine sail for ships and carried out a modeling study based on full-scale strain gauge data. The results indicated that, although the propulsion power contributed by the suction-based turbine sail is relatively small, they still play a significant role in fuel savings, especially under low-speed sailing conditions. Additionally, Y. Luan et al. (2015), through detailed numerical simulations of the flow field around the turbine sail, clearly pointed out that suction technology can significantly increase the lift coefficient while enhancing the flow field stability, providing crucial technical support for the optimization design of the turbine sail.

In conclusion, suction control technology has shown tremendous application potential in fields such as bridge structural stability, cylindrical flow control optimization, airfoil performance enhancement, and ship propulsion efficiency improvement by improving the flow field structure, suppressing boundary layer separation, reducing vortex strength, and lowering turbulence fluctuations. Specifically, parameters such as suction port position, size, and suction intensity have a significant impact on the flow field structure and force characteristics. The academic community has proposed a series of insightful recommendations regarding these factors. However, it should be noted that these factors do not act independently but interact and work together. Therefore, to assess their combined effects on the flow field more comprehensively and accurately, these factors should be considered as a whole for coordinated analysis. Notably, although several studies have addressed these factors, quantitative analysis of the combined effects of the suction port position and suction intensity, especially in the application of suction-type turbine sails in ship propulsion, remains insufficient. The suction-type turbine sail, a new type of ship auxiliary propulsion device, uses suction control technology to generate greater auxiliary thrust. The suction port position and suction intensity are not only directly related to the thrust output and energy consumption of the turbine sail but also profoundly affect the stability of the vortices and the state of flow separation. Therefore, investigating the combined effects of the suction port position and suction intensity on the performance of the turbine sail is of great theoretical value and can provide important insights into energy-saving and emission-reduction practices in the shipping industry. Based on this, this study focuses on the suction-type turbine sail in ship auxiliary propulsion systems, simplifying it to a two-dimensional model with a focus on the two key factors of suction port position and suction intensity. The aim was to systematically explore their combined effects on the flow field of turbine sails, offering new perspectives and insights for research and practice in the field.

2. Principles and Methods

2.1 Force Analysis of the Turbine Sail

A suction-type turbine sail is a novel wind-assisted propulsion device that optimizes the flow field characteristics around the turbine sail using suction control technology, thereby improving propulsion efficiency and reducing energy consumption. When the

airflow passes over the turbine sail, flow separation and vortex shedding often occur, which not only destabilizes the flow field, but also significantly increases the drag. To mitigate these adverse effects, the suction-type turbine sail was equipped with suction ports at the trailing edge, optimizing the flow attachment by applying suction, effectively suppressing flow separation, and significantly improving lift while reducing drag.

The main structure of the suction-type turbine sail includes a rotatable elliptical cylinder, suction ports, movable splitter plates, exhaust fans, and upper and lower end plates. The angle between the elliptical cylinder and incoming flow direction can be adjusted by rotating the cylinder, making it adaptable to different wind directions and sailing conditions, ensuring that the sail operates in an optimal state. Typically, suction ports are located on both sides of the cylinder trailing edge. The negative pressure created by the exhaust fan alters the local flow-field distribution, enhancing the flow attachment and increasing lift. The splitter plate is generally placed on one side of the trailing edge to shield one of the suction ports, helping control the flow direction and pressure distribution on the surface. Under the influence of suction, a significant pressure difference forms on the surface of the elliptical cylinder, generating a substantial lift, which is converted into thrust for propelling the ship forward. Additionally, the upper end plate primarily supports the exhaust system, whereas the lower end plate connects the sail body to the deck or supporting structure, ensuring that the suction-type turbine sail has sufficient structural rigidity and stability during operation. The design of the upper and lower end plates not only enhances the structural strength of the sail body, but also improves its resistance to torsion and overturning, ensuring that the device operates stably.

Compared to traditional or airfoil sails, suction-type turbine sails offer significant technical advantages. Its compact structure requires less space, generates more thrust, and has a stronger resistance to interference. By optimizing the suction parameters (such as suction intensity and suction port position) and sail body design, the suction-type turbine sail can significantly increase the wind energy utilization efficiency of ships. As an efficient wind energy utilization technology, suction-type turbine sails provide reliable technical support and development directions for energy saving, emission reduction, and green transformation in the shipping industry.

The geometry of the suction-type turbine sail is elliptical; the relevant definitions are shown in Fig.1. Assume that v_∞ is the uniform incoming flow, with the *x*-axis and *y*-axis representing the directions along and perpendicular to the incoming flow, respectively, as well as the directions of drag and lift. The intersections of the ellipse with the positive and negative *x*-axes are the trailing edge and leading edge, respectively, with the leading edge of the elliptical cylinder facing the wind. The intersections of the ellipse with the positive and negative *y*-axes are the upper and lower edges, respectively. A line connecting the center of the suction port to the center of the ellipse was drawn, and the angle between this line and the *x*-axis was defined as suction port position α. When the suction port center is at the trailing edge of the ellipse, α =0°, the counterclockwise rotation is positive. When the suction port center is at the upper edge of the ellipse, α = 90°The width of the suction port l_1, corresponds to the arc length for the central angle λ =10° of the ellipse. v_{in} is the suction velocity at the suction port, and the velocity direction is perpendicular to the surface of the elliptical geometric structure. Let β be the incoming flow angle of attack of an elliptical cylinder. When the incoming flow direction aligns with the long axis of the elliptical cylinder (*x*-axis), β = 0°, and the counterclockwise direction is positive.

A streamlined splitter plate was used to further improve the aerodynamic characteristics of the turbine sail. The position and width of the splitter plate are symmetric with respect to the *x*-axis and suction port. The function of the splitter plate is to reduce the flow separation and improve the stability and efficiency of the fluid flow. To comprehensively evaluate the aerodynamic performance of a suction-type turbine sail, dimensionless coefficients such as the lift coefficient C_L, drag coefficient C_D, lift-to-drag ratio *R*, and pressure coefficient C_P are typically used as performance indicators.

$$C_L = \frac{F_L}{0.5\rho V_\infty{}^2 A} \tag{1}$$

$$C_D = \frac{F_\mathrm{d}}{0.5\rho V_\infty{}^2 A} \tag{2}$$

$$C_P = \frac{P - P_\infty}{0.5\rho V_\infty{}^2} \tag{3}$$

$$R = \frac{C_L}{C_D} \tag{4}$$

In the equations, ρ represents the air density with a value of 1.225 kg/m^3, $V\infty$ denotes the magnitude of the freestream velocity, A represents the projected area perpendicular to the freestream direction, p is the pressure on the surface of the object, and P_0 is the static pressure under the freestream windward velocity.

The concept of suction intensity was introduced to represent the suction condition visually. Suction intensity is defined as the ratio of the suction velocity v_{in} to the uniform freestream velocity v_∞, denoted as γ, i.e., $\gamma=v_{in}/v_\infty$.

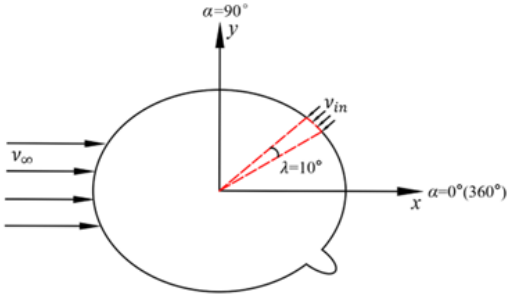

Fig 1. Schematic Diagram of the Suction-type Turbine Sail

2.2 Governing Equations and Numerical Methods

The governing equations for the flow field are the Navier (*N-S*) equations. Under typical conditions of ship navigation speed and encountered natural wind speed, air can be considered an incompressible fluid, allowing the energy conservation equation to be neglected. Therefore, when analyzing the flow field around the turbine sail, the governing equations include the mass conservation equation and momentum conservation equation, which in their two-dimensional form are as follows:

$$\frac{\partial u}{\partial x} + \frac{\partial v}{\partial y} = 0 \tag{5}$$

$$\rho\frac{\partial u}{\partial t} + \rho\nabla\cdot(u\boldsymbol{u}) = X - \frac{\partial p}{\partial x} + \frac{\partial \tau_{xx}}{\partial x} + \frac{\partial \tau_{yx}}{\partial y} \tag{6}$$

$$\rho\frac{\partial v}{\partial t} + \rho\nabla\cdot(v\boldsymbol{u}) = Y - \frac{\partial p}{\partial y} + \frac{\partial \tau_{xy}}{\partial x} + \frac{\partial \tau_{yy}}{\partial y} \tag{7}$$

In these equations, x and y represent the downstream and transverse directions, respectively. u and v represent the components of the velocity vector in the x and y directions, respectively. ρ is the fluid density. t is time. ∇·is the divergence of the velocity field. where u denotes the velocity vector. p is the pressure. τ denotes viscous stress. X and Y represent the body forces in the x and y directions, respectively.

The numerical simulations in this study were performed using FLUENT, with the SIMPLE algorithm used for pressure-velocity coupling, and a second-order upwind scheme was applied to discretize the convective terms. To fully simulate the effects of suction technology in ship propulsion, particularly considering the fluid intake and exhaust processes under actual suction effects as well as the complex separation flow and vortex shedding phenomena caused by the flow around the trailing edge of the turbine sail, the RNG k–ε turbulence model was selected for turbulence calculations.

In conducting the numerical simulations, several assumptions were made to simplify the calculations and improve the solution efficiency while maintaining the validity and feasibility of the results: (1) the wind field is steady with no wind speed gradients, (2) the effect of temperature is neglected, (3) the impact of ship inclination on the sail is neglected, and (4) the suction port area is treated as the suction surface.

3.Numerical Verification and Simulation Conditions

3.1 Computational Domain and Boundary Conditions

The aspect ratio of the ellipse was 5:4, with the length of the minor axis D being 2m. The overall computational domain is rectangular, as shown in Fig.2. The length and width of the computational domain are 50 and 20 times the length of the minor axis of the ellipse, respectively. The distance from the geometric center of the ellipse to the inlet boundary was 15D, to the outlet boundary was 35D, and to the upper and lower boundaries was 10D.

The boundary condition on the left side of the computational domain was a velocity inlet, the boundary condition on the right side was a pressure outlet, and the upper and lower boundaries were set as the symmetry planes. The remaining boundaries outside the elliptical suction port were set as no-slip walls, whereas the suction port location was set as a velocity outlet.

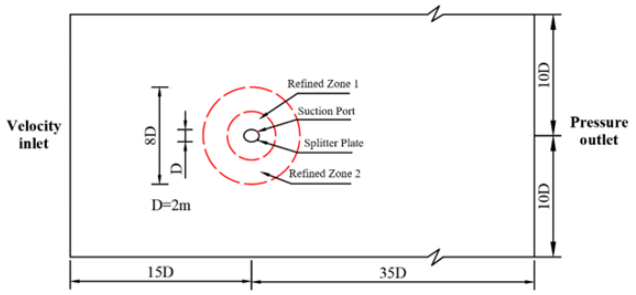

Fig 2. Flow Field Computational Domain

3.2 Grid Division Measures

A multi-region grid division strategy was adopted for the overall grid distribution, with a focus on structured grids. High-density grids were applied around the turbine sail to refine the flow calculations in the vicinity of the turbine surface and its wake region. To capture the flow characteristics near the turbine sail accurately, refined grid zones were implemented within the 4*D* and 8*D* regions around the turbine sail, as shown in Fig.2. For far-field regions, away from the turbine sail, a gradually coarsening transitional grid distribution is used, with grid sizes increasing from the core region to the far field, thereby achieving detailed flow field capture and efficient utilization of computational resources.

The boundary layer grids are arranged using an exponential growth method, with the thickness of the first layer (i.e., the cell height in the normal direction to the wall) strictly controlled based on the dimensionless wall distance *y*+ to meet the turbulence wall function calculation requirements. The total thickness and number of boundary layer grids were optimized through multiple iterations, capturing the flow gradient near the wall while avoiding computational resource waste due to excessive grid numbers. Based on the turbulence model, *y*+ was selected as 30, with 15 boundary layers and a growth rate of 1.15.

3.3 Grid Convergence Verification

In this study, a Reynolds number $Re = 3.678\times10^5$ and an angle of attack $\beta = -30°$were used for the simulation conditions to perform grid convergence verification. Based on the meshing strategy outlined in Section 2.2, five grid sizes were chosen for convergence verification. The lift and drag coefficients for these five grid sizes were compared with the simulation values from the literature (2015) as listed in Table 1. It is observed that there are certain differences in the lift and drag coefficients corresponding to different grid numbers. Grids 1 and 2 exhibited a higher lift coefficient, whereas the drag coefficient results exhibited small deviations. The results for grids 3–5 did not differ significantly. Considering both the computational accuracy and resource efficiency, grid 3 was selected for further analysis.

The total number of mesh cells in the computational domain is 1.117×10^5. The flow field mesh distribution is shown in Fig.3.

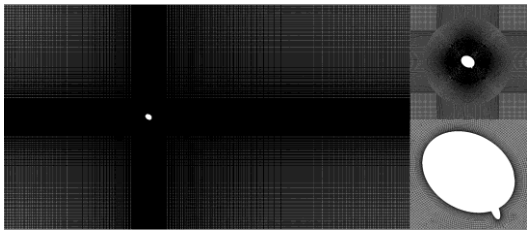

Fig.3. Mesh of Numerical Simulation

Tab. 1 Mesh independence study

Grid number	Mesh (ten thousand)	C_L		C_D	
		Value	Difference	Value	ifference
1	3.36	4.565	2.56%	0.886	3.69%
2	7.64	4.547	2.16%	0.889	3.36%
3	11.17	4.516	1.46%	0.895	2.71%
4	20.75	4.516	1.46%	0.896	2.60%
5	31.72	4.515	1.43%	0.896	2.60%
Y. Luan (2015)		4.451		0.920	

3.4 Numerical simulation verification

In this study, a Reynolds number *Re* = 3.678×105 and an angle of attack $\beta = -30°$ were used for the simulation conditions to perform numerical validation. The suction

port position was set at α = 25°. To investigate the impact of different suction intensities on the aerodynamic performance of the turbine sail, the suction intensity γ was varied within the range of 1.0 to 2.0, with a step size of 0.2. To verify the accuracy and reliability of the numerical method used, the lift coefficient C_L and drag coefficient C_D results from the simulations were compared with the numerical simulation results by Y. Luan (2015) and wind tunnel experimental data (1990). The results of numerical validation are presented in Fig.4.

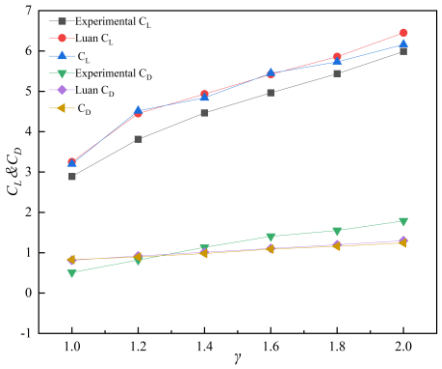

Fig.4. Numerical Simulation Verification Results

As shown in Fig.4, the overall trend of the numerical simulation results is consistent with that of the experimental results. Specifically, with the increase in suction intensity (γ), both the lift coefficient (C_L) and drag coefficient (C_D) of the turbine sail exhibited a gradually increasing trend. Notably, the numerical results obtained in this study were almost identical to those obtained by Luan, which further enhanced the reliability of the results. Although a slight difference was observed in the comparison, with the numerical simulation yielding a slightly higher lift coefficient (C_L) than the wind tunnel experimental data and a slightly lower drag coefficient (C_D), this discrepancy can be attributed primarily to a series of reasonable assumptions made during the two-dimensional numerical simulation process. The errors resulting from these assumptions were within the acceptable ranges. Therefore, the research approach used in this study provides an accurate representation of the aerodynamic characteristics of the turbine sail, offering reliable data support and a theoretical basis for further optimization of the turbine sail design.

3.5 Simulation Conditions

This study focused on the aerodynamic performance of a turbine sail installed on a bulk carrier using two-dimensional numerical simulations. The Reynolds number for the simulated conditions was set to Re = 1.36 ×10^6 based on real ship navigation data. The study specifically investigated the case with an attack angle of β=0°, with suction intensities (γ) ranging from 0.2 to 2.0, incremented by a step size of 0.2. To explore the influence of the suction port position on the performance of the turbine sail, the suction port position (α) was varied within the range of 5°–85°, with changes occurring every 10° in a counterclockwise direction. Through simulations, this study primarily analyzes the effects of suction intensity (γ) and suction port position (α) on the lift coefficient (C_L) and drag coefficient (C_D) of the turbine sail, and further examines how changes in the suction port position (α) affect the flow field structure around the turbine sail.

4. Results and Analysis

4.1 Combined Effect of Suction Port Position and Suction Intensity on the Lift and Drag Coefficients of the Turbine Sail

To comprehensively investigate the effects of suction intensity (γ) and suction port position (α) on the aerodynamic performance of the turbine sail, this study systematically plots the variations in the lift coefficient (C_L), drag coefficient (C_D), and lift-to-drag ratio (R) with respect to the suction intensity (γ) and suction port position (α) through two-dimensional numerical simulations, as shown in Fig. 5–7. These plots visually revealed the distribution trends and variation characteristics of the aerodynamic performance of the turbine sail under different suction parameter configurations.

As shown in Fig.5, both the suction intensity (γ) and suction port position (α) had a significant impact on the lift coefficient (C_L) of the turbine sail. Overall, C_L increases noticeably with an increase in γ, but the rate and nature of this increase vary depending onα, reflecting the critical role ofα in controlling the flow field.

When $\alpha \leq 45°$ and $\gamma < 0.6$, the variation in α has a more pronounced effect on C_L. Specifically, under a constant γ, asα moves from the rear edge (where α is small) towards the leading edge, C_L initially decreases and then increases. When α is less than 15°, suction does not effectively influence the primary separation region of the flow field, leading to a relatively poor control

performance when γ is low. An ideal control effect can only be achieved by increasing γ. In the range of α = 15°–45°, C_L increases noticeably with α, and with the increase in γ, C_L also shows a clear upward trend. This suggests that at Re = 1.36 × 10^6, setting α between the rear edge and the leading edge, along with increasing γ, is beneficial for increasing C_L and achieving better control performance.

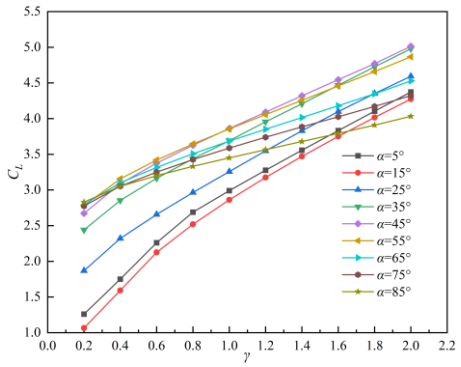

Fig 5. Lift Coefficient under the Combined Effect of Suction Intensity and Suction Port Position

When α > 45°, C_L increased with γ. This is because of the stronger suction, which facilitates the reattachment of the fluid to some extent, suppresses vortex shedding at the rear, and improves the local flow field stability. However, compared with the α = 45° case, the increase in C_L was slower. This indicates that as α moves closer to the leading edge, the control effect of increasing γ weakens. It is also observed that when α > 45°, under constant γ, C_L decreases as α moves closer to the leading edge. This is primarily because the suction disturbance, when positioned near the leading edge, prematurely extracts the fluid, weakening the flow-cofigntrol effect on the main separation region of the flow field, which reduces the overall lift performance.

It is noteworthy that when α = 35°–55°, C_L reaches its peak, indicating the optimal suction effect in this range. Within this range, suction effectively suppressed vortex separation, stabilized the flow field structure, and generated the maximum aerodynamic force in the lift direction. This is because the suction position in this range can fully influence the primary separation region of the fluid, effectively improving the boundary-layer attachment state and reducing the dissipation of fluid kinetic energy, thus maximizing the lift performance. When $\alpha \leq$ 25°, suction does not sufficiently affect the main flow-field region, leading to a limited improvement in the flow attachment. When $\alpha \geq$ 65°, suction disturbance occurs too early, making it difficult for the fluid to reattach after separation, further reducing the lift performance. Therefore, under most suction intensities, α = 35°–55° exhibits a higher lift coefficient, indicating that the suction configuration in this range is the ideal setup for optimizing the aerodynamic performance of the turbine sail.

The conclusions above are further validated by the pressure and vorticity field distributions. When α is between 35° and 55°, suction significantly delays the onset of the primary separation point, creates a more favorable pressure gradient for lift generation, weakens the wake vortices, and results in a more stable flow field. In contrast, when α is too small or too large, the suction port becomes misaligned with the main separation region, reducing the effectiveness of flow disturbance or even triggering flow instability, which ultimately diminishes the control performance.

In conclusion, the interaction between γ and α significantly affected the C_L of the turbine sail. By appropriately selecting the suction port position, especially within the α =35° to 55° range, and increasing γ, the boundary layer separation can be effectively controlled, the flow field structure can be optimized, and the lift performance of the turbine sail can be maximized.

Both the suction intensity (γ) and suction port position (α) had a significant impact on the drag coefficient (C_D) of the turbine sail. Different combinations of suction parameters lead to changes in the flow-field structure and boundary-layer distribution, which in turn affect the drag characteristics of the turbine sail. As shown in Fig.6, C_D exhibited a clear nonlinear relationship with γ and α.

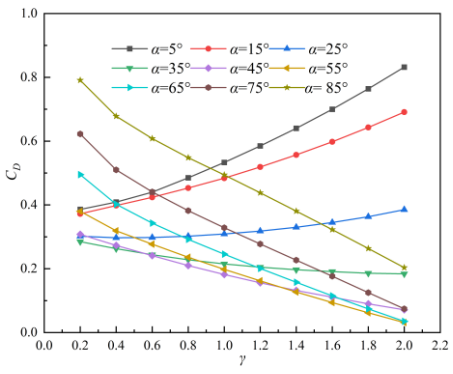

Fig.6. Drag Coefficient under the Combined Effect of Suction Intensity and Suction Port Position

When $\alpha \leq$ 25°, C_D decreases as α increases but increases as γ increases. This is because, when α is closer to the rear edge, the suction control has not yet fully

affected the primary separation region of the flow field. Meanwhile, as α moves further from the rear edge, the disturbance in the flow near the splitter plate intensifies, thereby generating new vortices around the splitter plate. Additionally, as γ increased, the disturbance effect of the suction port at the rear edge increased, leading to a decrease in the stability of the fluid at the rear edge, which caused C_D to increase.

When α = 35°–55°, C_D shows a clear decreasing trend as γ increases and remains at a generally low level. This is because within this α range, suction control helps improve the boundary layer flow state and effectively suppresses flow separation, thereby reducing the drag coefficient. It was also observed that as γ increased, C_D did not decrease monotonically but exhibited fluctuations with both increases and decreases. This further suggests that this α range corresponds to the critical region for boundary-layer flow separation on the turbine sail surface, and the effectiveness of suction control is particularly sensitive to changes in γ.

When $\alpha \geq 65°$, the drag coefficient (C_D) continues to show a significant decreasing trend with increasing suction intensity (γ). This indicates that suction near the trailing edge still plays a role in suppressing vortex shedding and can effectively reduce drag. However, it is important to note that despite the clear drag reduction, the lift coefficient (C_L) remains relatively low in this range of α. This suggests that suction control at such positions fails to effectively improve boundary layer attachment in the mid and trailing edge regions, limiting the overall flow control effectiveness and resulting in reduced aerodynamic performance of the turbine sail. Furthermore, analysis of the pressure and vorticity field distributions provides deeper insight into how α and γ influence C_D. When α is positioned too close to the upper edge, it tends to generate asymmetrically distributed vortices. While this can contribute to drag reduction, it compromises flow field stability. Therefore, it is not recommended to place the suction port in this region.

In conclusion, the combined effects of α and γ on C_D followed a clear pattern. Based on the results shown in Figs. 5 and 6, it can be concluded that α = 45°–65° is the optimal range for improving both the lift and drag performance of the turbine sail, providing effective design guidelines and optimization strategies for practical engineering applications.

Additionally, to more comprehensively evaluate the impact of α on the turbine sail performance, it is essential to not only analyze C_L and C_D, but also further investigate the lift-to-drag ratio (R), which is a key performance indicator. R is an important parameter for assessing the aerodynamic performance of the turbine sail. A higher R indicates that a greater lift can be generated for the same drag loss, which is significant for evaluating the propulsion efficiency of the turbine sail. The results for the lift-to-drag ratio under the combined effects of suction intensity and suction port position are shown in Fig.7.

As shown in Fig.7, the impact of the suction intensity (γ) and suction port position (α) on the lift-to-drag ratio (R) exhibited a clear dynamic pattern. When γ was small, the effect of α on R was relatively limited. This is because a small γ value is insufficient to significantly alter the flow-field structure, resulting in negligible changes in R. However, as γ increases, the influence of α on R becomes more pronounced, particularly when γ > 1.6, where the differences in R between different α values become more significant. At γ = 2.0, R reaches its maximum value of 154.97 at α = 55° and its minimum value of 5.26 at α = 5°, with a difference of nearly 30 times between the two values.

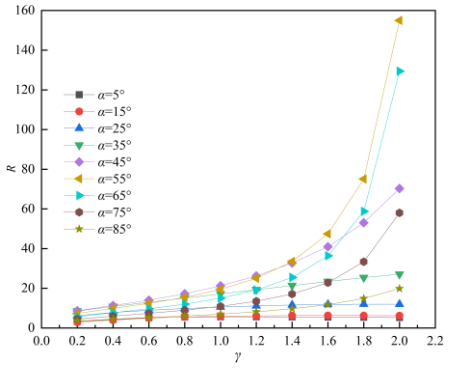

Fig.7. Lift-to-Drag Ratio under the Combined Effect of Suction Intensity and Suction Port Position

Specifically, when γ > 1.6, the effect of α on R was more noticeable. When $\alpha \leq 25°$, close to the rear edge, the airflow adheres well to the turbine sail surface, guiding the air to pass smoothly over the surface and reducing the formation of the local vortices. At this point, the lift performance is relatively high; however, because α is too close to the rear edge, the airflow does not generate strong vortices or significant flow separation. Consequently, the local flow speed increased, and the

fluid pressure distribution became uneven, causing an increase in the drag. This imbalance between lift and drag leads to a relatively low R.

When α = 45°–55°, α effectively balances lift and drag, allowing the airflow to pass more smoothly over the turbine sail surface while forming a stable vortex structure. Suction control suppresses boundary layer separation, delays the movement of the flow separation point towards the leading edge, and reduces the turbulence intensity and vortex size, which significantly decreases the drag. Meanwhile, the lift remains relatively high within this range, resulting in optimal aerodynamic performance for R in the range of α = 45°–55 °. Although R was also high at α = 65°, the vortex structure became larger and asymmetric, causing instability in the flow field. Therefore, the R value was not the best choice.

When $\alpha \geq 75°$, the suction effect primarily influences the leading edge. Although suction still helps reduce drag to some extent, the flow separation increases, leading to stronger local turbulence, which weakens the drag reduction effect. Additionally, from the pressure and vorticity fields, it is evident that the asymmetry of the vortices and the increased strength of the wake vortex reduce lift, resulting in poorer performance of R。

The variation in α directly influences the fluid characteristics on the turbine sail surface, including the boundary layer attachment, vortex formation, and tail vortex distribution. A distribution of α that is too close to the rear or leading edge will negatively affect R, making the rational selection of α particularly important. Within an appropriate range, suction technology can effectively control the flow separation and vortex formation while balancing the relationship between lift and drag, thereby optimizing R.

From the analysis of the variation patterns of C_L, C_D, and R, it is clear that synergy between α and γ is crucial for optimizing the aerodynamic performance of the turbine sail. As noted in the previous analysis, the larger the value of γ, the more pronounced the changes in R across different α values and the more evident the control effect on the flow field. Therefore, to further explore the optimization strategy for suction control, a more in-depth study and analysis of the variation patterns under the typical condition of γ = 2.0 will be conducted in Sections 3.2, 3.3, and 3.4.

4.2 Effect of Suction Port Position on the Pressure Coefficient of the Turbine Sail

A systematic analysis of the pressure coefficient (C_p) distribution under different α values was conducted to investigate the influence of the suction port position (α) on the pressure distribution of the turbine sail, a systematic analysis of the pressure coefficient (C_p) distribution under different α values was conducted. The pressure coefficient (C_p) is a key parameter for describing the pressure distribution of airflow on the turbine sail surface, and its variation directly affects the lift and drag characteristics of the turbine sail. The variation curves of C_p under different α values are shown in Fig.8, where the circumferential angle θ of the elliptical cylinder cross section of the turbine sail is used as the coordinate. Here, θ = 0° (or θ = 360°) corresponds to the windward face of the elliptical cylinder (i.e., the negative half of the x-axis) and θ = 180° corresponds to the leeward face (i.e., the positive half of the x-axis).

As shown in Fig8, the suction led to a sharp pressure drop (C_p). This phenomenon indicates that suction control has a significant impact on the pressure distribution of the flow field, resulting in a considerable reduction in the pressure in the localized regions. This pressure reduction primarily reflects the effect of suction on momentum change in the flow field. By altering the fluid velocity within the boundary layer, the boundary layer thickness was reduced, and the attachment ability of the fluid in the suction area was enhanced, thus delaying the occurrence of flow separation.

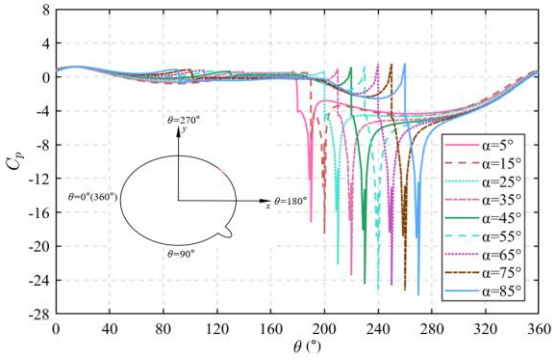

Fig.8.Variation Curve of C_p under Different Suction Port Positions

By examining the variations in the curves in the figure, it can be further observed that when $\alpha \leq 25°$, suction control effectively reduced the local pressure at the rear edge, improving the flow attachment state of the

boundary layer at the rear edge and enhancing the overall stability of the flow field. However, because α was too close to the rear edge, the pressure drop was relatively small, and the suction control effect was not ideal. As discussed earlier, suction control in this case did not significantly improve the lift coefficient (C_L) and drag coefficient (C_D), and the lift-to-drag ratio (R) remained low. Therefore, suction near the rear edge is not ideal.

When $\alpha \geq 65°$, the suction effect was primarily concentrated near the leading edge of the turbine sail. Although this configuration significantly reduces C_p and achieves effective suction control, a potential issue arises: the lowest pressure point is located near the leading edge, creating a large gap between it and rear edge. This can easily result in an adverse reverse pressure gradient between the leading and trailing edges, exacerbating the turbulent characteristics at the rear edge and causing a premature flow separation. Ultimately, this negatively affects the overall performance of the turbine sail, thereby reducing its propulsion efficiency and stability.

However, when α = 45°–55°, suction control not only significantly reduces the local C_p on the surface of the turbine sail, forming a moderate low-pressure zone at the rear edge, but also maintains a uniform overall pressure gradient in the flow field. This pressure distribution, in addition to increasing C_L, can suppress turbulence and tail vortex instability, and reduce C_D. Therefore, suction control in this range provides the best performance in terms of the lift-to-drag ratio and flow field stability, confirming that it is the ideal suction port position.

4.3 Effect of Suction Port Position on the Flow Field Flow

To further investigate the specific impact of the suction port position on the fluid flow characteristics around the turbine sail, this study conducted a systematic analysis of the flow field surrounding the turbine sail under different suction port positions. The instantaneous velocity streamline patterns on the turbine sail surface at different suction port positions are shown in Fig.9, and the variations and trends of the streamlines are analyzed in detail to reveal the influence of the suction port position on the flow characteristics and flow field control.

As shown in Fig.9, the variation in α exhibited a clear pattern in its impact on the fluid flow characteristics around the turbine sail. The change in α not only affects the suppression of flow separation, but also influences the generation and dis-tribution of vortices, as well as the intensity of disturbances in the wake region and the stability of the flow field.

When $\alpha \leq 25°$, the suction effect was primarily concentrated in the rear edge region of the turbine sail. At this point, suction has a strong ability to guide the fluid within the boundary layer, helping to reduce the pressure in the boundary layer and ensuring that the fluid adheres more closely to the surface of the turbine sail, thereby suppressing the flow separation. However, because α is relatively close to the rear edge, the suction effect is limited, and the flow-field optimization in the upper-middle region is insufficient, leading to a constrained flow-field control capability. Regarding vortex generation and distribution, small suction angles primarily affected the initial flow state in the wake region. At this point, the vortices in the wake region are weak and uniformly distributed with low disturbance intensity, indicating a relatively stable flow field. However, the generation of weak vortices also suggests insufficient momentum exchange in the wake region, preventing the suction effect from significantly improving thrust. In terms of disturbances and stability in the wake region, although small suction angles maintain the flow field stability in the wake region, this stability is more a result of inadequate momentum exchange than that of the optimized flow. Overall, the suction control effect on the flow field was limited, with a relatively low system energy consumption and weak thrust improvement.

When α = 35°–55°, positioned between the leading and rear edges, the suction effect not only covers the leading-edge region of the turbine sail, but also effectively extends to the middle and rear edge regions. This broader distribution range is more conducive for optimizing the flow state across the entire surface of the turbine sail. The suction port significantly reduced the boundary layer pressure, further suppressing the flow separation and substantially improving the fluid flow state. Regarding the vortex generation and distribution, under medium suction angles, the vortex strength in the wake region was moderate, and the vortex structure generated was clear and evenly distributed. The momentum exchange in the wake region was enhanced, and the vortex disturbance was moderate, achieving a good balance between thrust improvement and flow

field stability. At this point, suction optimizes the flow state in the wake region and enhances the thrust output efficiency of the turbine sail. The advantages of medium suction angles are particularly evident in terms of the disturbances and stability in the wake region. The disturbance intensity in the wake region is moderate, avoiding the insufficient disturbance observed with small suction angles and the instability caused by excessive disturbance at large suction angles. Overall, within this α range, both the thrust output and overall flow field stability were significantly improved, making it the optimal suction port position.

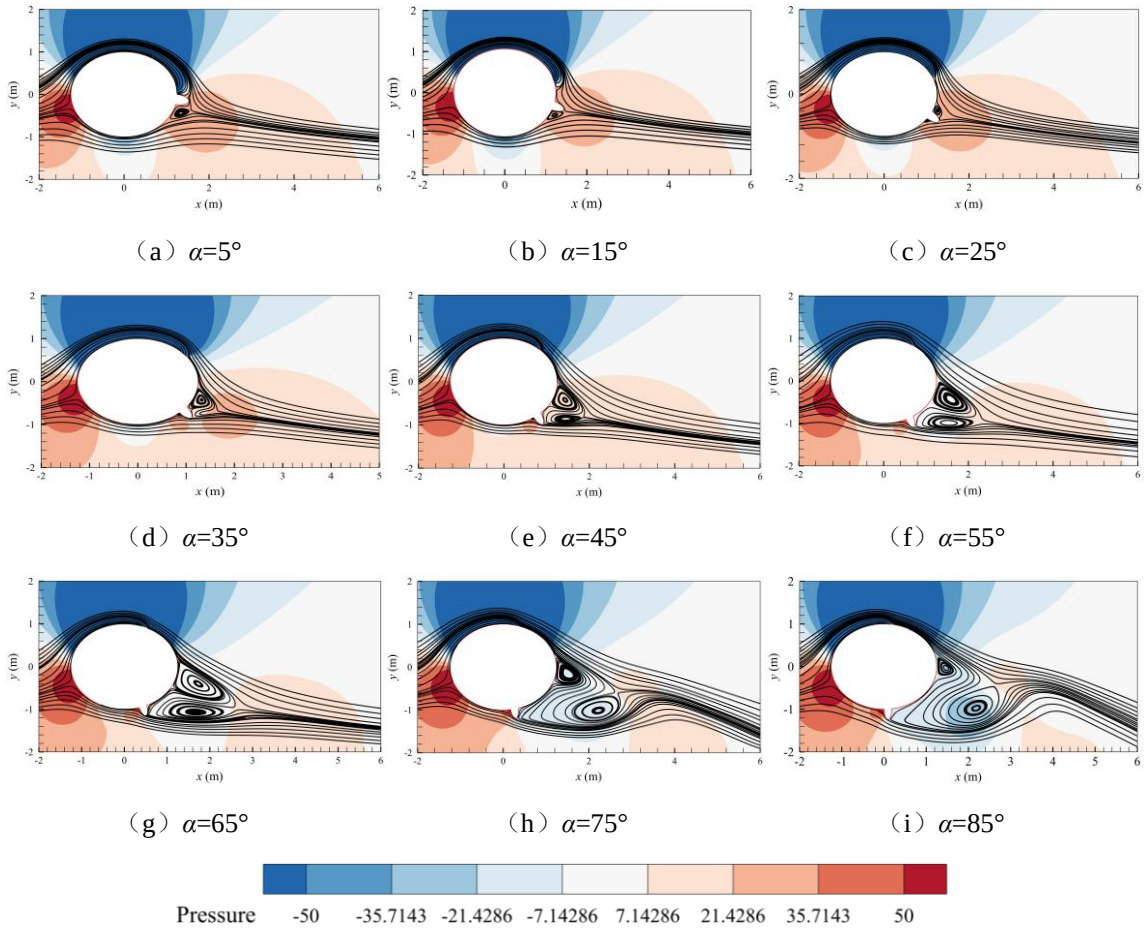

Fig.9. Instantaneous Streamlines on the Surface of the Turbine Sail under Different Suction Port Positions

When $\alpha \geq 65°$, the suction effect was primarily concentrated near the leading edge of the turbine sail. At this point, the suction's ability to guide the fluid in the middle and rear edge regions weakens, while its ability to suppress fluid separation in the leading edge region strengthens, significantly reducing the flow separation in that region. However, because α is too close to the leading edge, the overall flow-field pressure distribution becomes uneven, which may lead to insufficient flow optimization in the rear and middle regions. Regarding the vortex generation and distribution, under large suction angles, the vortex strength in the wake region was significantly enhanced, and the disturbance frequency increased. While enhanced vortex generation can further improve the thrust output, the stability of the wake region flow field significantly decreases, potentially triggering irregular vortex disturbances and leading to increased energy losses. In terms of disturbances and stability in the wake region, large suction angles caused significantly stronger disturbances, and the wake region exhibited considerable instability, possibly generating high-frequency turbulence. In this case, although the thrust is increased, the significant reduction in the flow field stability and the increase in the system energy consumption negatively impact the reliability and safety of navigation.

In summary, the effect of α on the flow field around a turbine sail was significant. When $\alpha \leq 25°$, the flow field was relatively stable, but the thrust improvement was limited. When $\alpha \geq 65°$, while the thrust is increased, the flow field stability significantly decreases, leading to increased energy consumption, which limits the practical engineering significance. In contrast, when α = 35°–55°, positioned between the leading and rear edges, the suppression of fluid separation, optimization of vortex

generation and distribution, and control of disturbances in the wake region all reach optimal levels. This range is the ideal suction-port position.

4.4 Effect of Suction Port Position on the Wake Vortex Structure in the Flow Field

To further elucidate the influence of α on the wake characteristics of the turbine sail and its variation patterns, this section provides a detailed discussion of vortex shedding in the wake of the turbine sail. By analyzing the structure and variation of wake vortex shedding, the mechanisms by which α affects key processes such as momentum exchange, vortex generation, and energy dissipation in the flow field can be more intuitively understood. The vortex shedding structure in the wake of the turbine sail at different α values is shown in Fig.10.

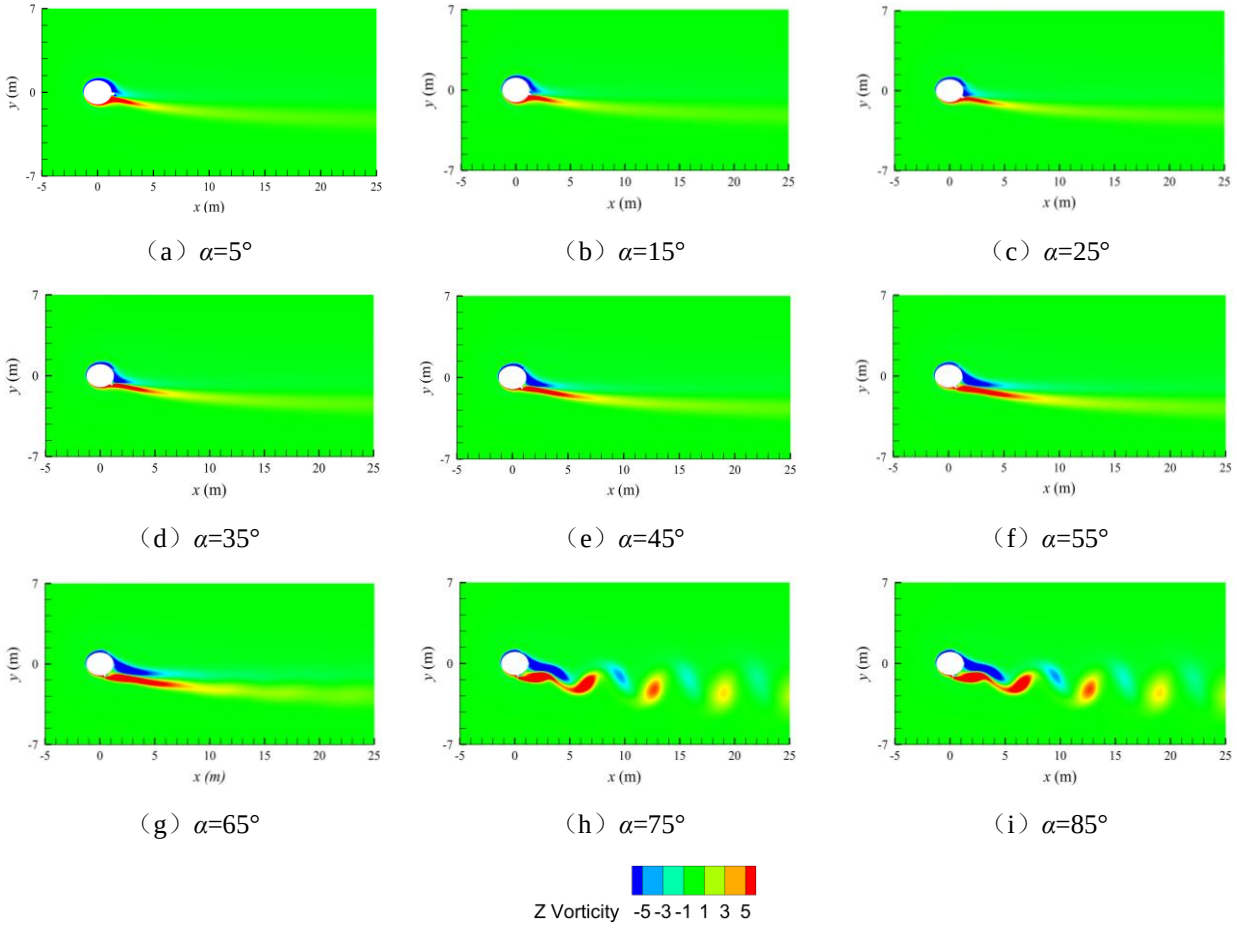

（a）α=5° （b）α=15° （c）α=25°

（d）α=35° （e）α=45° （f）α=55°

（g）α=65° （h）α=75° （i）α=85°

Fig.10. Wake Vortex Shedding Structure of the Turbine Sail under Different Suction Port Positions

By comparing the effects of different α values on the wake vortex distribution and vortex shedding patterns under the same γ, it can be observed that when $\alpha \leq 25°$, the suction disturbance in the wake is relatively weak in both the range and intensity. The vortex generation in the wake region was weak, and the overall flow field exhibited good stability with a smooth wake and limited energy dissipation in the wake region. However, because γ primarily influences the rear edge of the flow field, it is difficult to significantly enhance the momentum exchange and fluid reattachment ability in the wake region, which results in limited thrust improvement. Although the flow field stability was high, the overall optimization effect was insufficient.

When α = 35°–55°, positioned between the leading and rear edges, the suction effect on the wake vortices reaches an optimal balance. The disturbance intensity was moderate, and momentum exchange and fluid reattachment in the wake region were significantly improved. Within this range, the energy dissipation was moderate and the vortex distribution in the wake region was neither too intense nor too mild. At this point, α effectively enhances the stability of the flow field.

When $\alpha \geq 65°$, as α increases further, the suction disturbance becomes significantly stronger, leading to vortex shedding in the wake region and chaotic wake structures. While stronger suction disturbances can suppress local flow separation and increase lift, excessive disturbances exacerbate instability in the wake region, causing the vortex distribution in the flow field to

fluctuate dramatically, accompanied by significant energy dissipation. The overall flow field exhibited irregular vortex shedding characteristics, leading to a decrease in thrust efficiency and system stability. Therefore, excessively large suction angles are detrimental to further optimization of turbine sail performance.

In conclusion, the influence of different α values on the wake vortex shedding structure of the turbine sail follows a significant pattern: when $\alpha \leq 25°$, the flow field is stable, but thrust improvement is limited; when α = 35°–55°, positioned between the leading and rear edges, the balance between suction disturbance and flow field stability is optimal, resulting in significant thrust improvement; when $\alpha \geq 65°$, near the leading edge, the excessive disturbance causes a significant decrease in the flow field stability, degrading the overall performance. Based on this analysis, the optimal suction port position is α = 35°–55°, where suction can effectively optimize the wake structure and significantly enhance propulsion performance, yielding the best application results.

5. Conclusion

This study systematically explores the combined effects of suction intensity and suction port position on the aerodynamic performance of an exhaust-type turbine sail, revealing the underlying mechanisms and patterns of how these parameters optimize the turbine sail performance. The focus is on analyzing the flow field characteristics and vortex structure changes at a suction intensity of γ = 2 under different suction port positions, providing important theoretical foundations and practical guidance for the optimization design of turbine sails. The following conclusions were drawn.

(1) The variation in suction intensity can significantly affect the lift and drag characteristics of the turbine sail, thereby impacting its lift-to-drag ratio performance. An appropriate suction intensity enhances the flow attachment to the turbine sail surface, delays the flow separation, and improves the overall aerodynamic efficiency of the turbine sail. By appropriately designing the suction intensity parameters, the aerodynamic performance of the turbine sail can be optimized under various navigation conditions.

(2) The suction port position has a particularly significant impact on the flow field structure around the turbine sail, particularly in terms of flow attachment, fluid separation, and wake vortex shedding characteristics. The results showed that when the suction port position was between the leading and trailing edges, the turbine sail exhibited the best aerodynamic performance. In this range, suction effectively optimizes the flow attachment, suppresses flow separation, and significantly improves the dynamic balance between lift and drag, thereby achieving the maximum lift-to-drag ratio. Additionally, the periodicity of the vortex shedding in the wake region was enhanced, and its distribution became more regular. The disturbances in the wake region were significantly reduced, and the overall flow field structure became more stable. This not only enhances the aerodynamic efficiency of the turbine sail, but also significantly improves its wind resistance stability, providing a clear direction for the optimization of exhaust-type turbine sails.

In summary, this study comprehensively reveals the effects of suction intensity and suction port position on the performance of the exhaust-type turbine sail, enriching the theoretical framework of turbine sail aerodynamic characteristics and flow field control mechanisms. It provides crucial theoretical support and a technical reference for the design and application of exhaust-type turbine sails. The results of this study offer an optimization basis for the practical application of exhaust-type turbine sails in wind-assisted navigation, and are of great significance for promoting energy saving, emission reduction, and green transformation in the shipping industry.

Future research could focus on the following aspects.

(1) Analysis of unsteady flow characteristics of exhaust-type turbine sails under different incoming attack angles under complex sailing conditions to enhance their performance in dynamic environments.

(2) Exploration of the synergistic control mechanism of suction and blowing combined, investigating its comprehensive optimization effect on aerodynamic performance under different flow field conditions.

(3) Comprehensive consideration of actual ship operating conditions, integrating intelligent control technologies, and IoT systems to develop more adaptive and efficient optimization control strategies for turbine sails, driving their widespread application in energy-saving and emission-reduction efforts in the shipping industry.

References

J. Zhang. (2024), Application and prospects of new energy technologies in ships, Ship Materials & Markets, 32(6), pp.91–93

G Jordan, M Henry. (2024), IMO2020 regulations accelerate global warming by up to 3 years in UKESM1. Earth's Future,12(8), e2024EF005011

Z Li, J Tang. (2024), Circulation-controlled wind-assisted ship propulsion: Technical innovations for future shipping industry decarbonization, Energy Conversion and Management, 319118976-118976

H Wang, C Li, C Zuo, et al. (2024), Computational Fluid Dynamics Investigation of the Spacing of the Aerodynamic Characteristics for Multiple Wingsails on Ships, Journal of Marine Science and Engineering, 12(6),985

H Yan, S Wang, Y Han, et al. (2023), Numerical simulations on flow control of the long hanger around a bridge tower based on active suction and blowing method, Physics of Fluids, 35(11),

W Liu, Y Liu, D Shang, et al. (2024), The flow-induced structural vibration noise suppression mechanism of a wing–plate model by the junction suction and trailing edge blowing. Journal of Sound and Vibration,578,118340

Y Liu, S Fei, D Shang, et al. (2020), The method to suppress the hydrodynamic noise from a sail hull model by the suction technique, Institute of Noise Control Engineering, 261(2), pp4344-4355

X. Shi, J. Sun, D. Huang, et al. (2021), Effect of Boundary Layer Suction on the Vortex Shedding Structure and Force on a Cylinder in Crossflow, Journal of Thermal Power Engineering, 36(6), pp63–69

A. Tang, S. Tao. (2016), Experimental Study on Vortex-Induced Vibration Characteristics of a Cylinder under Suction, Journal of Huazhong University of Science and Technology, 44(02) pp.97–101

N. Chen. (1994), Numerical Study of the Effect of Suction on Unsteady Separation Flow of a Cylinder Acta Aerodynamica Sinica, 12(03) pp.288–294

J Fransson, P Konieczny, P Alfredsson, et al. (2004), Flow around a porous cylinder subject to continuous suction or blowing, Journal of Fluids and Structures, 19(8), pp1031-1048

W. Chen, D. Xin, F. Xu, et al. (2013), Suppression of vortex-induced vibration of a circular cylinder using suction-based flow control, Journal of Fluids and Structures, pp4225-39

W. Chen, B. Li, C. Xu, et al. (2023), Effects of distributed suction through the porous side-walls of a square cylinder on separation and wake flows, European Journal of Mechanics / B Fluids, pp991-16

C. Liu (2017), Experimental Study on the Mechanism of Suction Control in Bluff Body Flow Fields, PhD diss, Harbin Institute of Technology,

Y Zhong, H Ma, D Yun, et al. (2022), Effects of different suction angles on flow structures and dissipation in the wake of a circular cylinder. Ocean Engineering, 266,112521

Y Zhong, H Ma, H Li, et al. (2022), Influence of surface suction on wake characteristics behind a circular cylinder, Journal of Visualization, 25(4), pp767-790

L. Wang, M. A. Mahbub, R. Shafiqur, et al. (2022)., Effects of blowing and suction jets on the aerodynamic performance of wind turbine airfoil, Renewable Energy,19652-64

W Zhang, Z Zhang, Z Chen, et al. (2017), Main characteristics of suction control of flow separation of an airfoil at low Reynolds numbers, European Journal of Mechanics-B/Fluids, 65, 88-97

D Ma, G Li, M Yang, et al. (2018), Research of the suction flow control on wings at low Reynolds numbers, Proceedings of the Institution of Mechanical Engineers, Part G: Journal of Aerospace Engineering, 232(8),1515-1528.

S. Gao(2017), Numerical Study to Improve the Aerodynamic Performance of Wind Turbine Airfoils, Northeast Electric Power University,

K. Balaji, J. G. W. (2021). Gowda, Enhancement of Aerodynamic Efficiency of Aerofoil Using Improved Blowing and Suction System, Advances in Science and Technology-Research Journal,15(2),116-126

A. Farhadi, G. E. Rad, H. (2017). Emdad, Aerodynamic Multi-Parameter Optimization of NACA0012 Airfoil Using Suction/Blowing Jet Technique,Arabian Journal for Science and Engineering, 42(5),1727-1735

И Корнилов. (2020), Combined Blowing/Suction Flow Control on Low-Speed Airfoils, Flow, Turbulence and Combustion, 106(1),81-108

K Dohyun, L Minhyeong , M Ehsan, et al. (2024), Coordinated suction and blowing of a cylinder array for thrust generation, Journal of Fluid Mechanics, 979(426),A26-A26.

W. Chen, Y. Guo. (2020). Flow Control around a Cylinder Based on Active Suction and Blowing, Acta Aerodynamica Sinica, 38(5), 989–995

C James, V Marco, G Richard, et al. (2021), Numerical optimisation of a ship wind-assisted propulsion system using blowing and suction over a range of wind conditions, Ocean Engineering, 240

O Guerri, E Liberge, A Hamdouni, (2016) Numerical Simulation of the Turbulent Flow around an Oval-Sail[J]. Journal of Applied Fluid Mechanics,9(6):pp2009-2023.

M Ghorbani, P Slaets, J Lacey. (2024) Sensor-based modelling of suction sails to integrate into a numerical simulation tool for a wind-assisted vessel and its application to green shipping[J]. Ocean Engineering, 311: 118937.

Y. Luan, Y. Hu, Z. Li. (2015), Aerodynamic Analysis of Suction-Type Turbine Sails, Ship Engineering, 37(02),21-23,49

G. Li, H. Luo, Z. Tan, et al. (1990), Energy-Saving Ship

Design. National Defense Industry Press,

Received **20 March 2025**

1st Revised **23 May 2025**

Accepted **18 June 2025**